LAND SALINIZATION DYNAMICS BASED ON FEATURE SPACE COMBINATIONS FROM LANDSAT IMAGE IN TONGYU COUNTY, NORTHEAST CHINA

F. Huang*, P. Wang, Y.Liu, H.Y. Li

Key Laboratory of Geographical Processes and Ecological Security in Changbai Mountains, Ministry of Education, School of Geographical Sciences, Northeast Normal University, Renmin Street, Changchun, China- (huangf835, wangp666) @nenu.edu.cn, (1324777979,1611279624) @qq.com

Commission III,WG III/1

KEY WORDS: Salinization, Feature Space, Albedo, Modified Soil Adjusted Vegetation Index, Salinity Index, Landsat Image

ABSTRACT:

Land salinization is one of the most common land degradation processes. Tongyu county exemplifies all the forms of land degradation in Northeast China and is prone to land salinization due to its fragile physical conditions. In this study, Landsat remote sensing images are adopted to invert surface albedo, MSAVI (modified soil adjusted vegetation index), and salinity index (SI) data. The feature space models of albedo-SI and MSAVI-SI, considering the bare soil and vegetation information respectively, are constructed and compared. Land salinization changes for the period of 1998-2017 are investigated using the salinization monitoring index (SMI) and salinization detection index (SDI) extracted from the feature space models. Our results show that the land salinization situation in Tongyu county have tended to improve, associated with the biological, ecological and engineering means for the degraded land rehabilitation. The feature space models is applicable for the extraction of salinization information, and albedo-SI may evaluate land salinization levels with higher accuracy.

1. INTRODUCTION

Land salinization is one of the most common land degradation processes (UNEP, 1991), which often occurs particularly in arid or semiarid areas (Masoud and Koike, 2006), due to low rainfall, high evapotranspiration rates. The soil textural characteristics may impede the washing out of the salts which subsequently built-up in the soil surface layers. Land salinization poses threats on ecosystem and environment obviously (Line et al., 2010; Allbed et al., 2014; Peng et al., 2018). Accumulation of soluble salts in the soil is one of the main limiting factors for agriculture. Dynamic monitoring of land salinization by knowing when, where, and how salinity may occur is significant for proper management of soil and water resources (Ding and Yu, 2014; Fan et al., 2015).

Compared to the laboratory analysis methods, remote sensing provides significantly powerful approach for large-scale characterization and monitoring of land salinization. The spectral characteristics of saline soils are theoretical basis for remote sensing monitoring. A positive relationship between soil reflectance in visible-near infrared-shortwave infrared bands and soil salinization has been found. Visual interpretation and automated classification considering soil salinity, groundwater, and other auxiliary factors are two main methods to identify salinization information from remote sensing images. Many satellite-based indices derived from the reflectance in different spectral bands have been utilized for monitoring salinization. Multiple indices comprising of spectral bands in different combinations were calculated and compared to identify salinized soils (Guo et al.,2019). The characteristic information of feature spaces has been widely applied to estimate soil salinity and evaluate surface evapotranspiration, soil moisture, crop moisture content, and desertification dynamics (Allbed and Kumar, 2013). For instance, albedo and salinity index (SI), modified soil adjusted vegetation index (MSAVI) and Wetness Index (WI), and MSAVI–SI were used to construct different feature space models and quantify the salinization (Ha et al., 2009; Ding et al.,2013; Zhang et al.,2016).

Tongyu County is in the western fringe of the Songnen Plain, which is the biggest distribution area of soda saline land in China (Gu et al., 2010). This county is highly prone to salinization/alkalization owing to an abundant supply of salts and a shallow groundwater table (Gao and Liu, 2010). Previous researches had paid attention to the detailed spatio-temporal transformation relationship between saline land and other land cover types and long-term hydrological process of the Songnen Plain.

In this paper, surface albedo, MSAVI and salinity index feature spaces based on Landsat TM and OLI images were constructed and compared. The salinization monitoring index (SMI) and salinization detection index (SDI) derived from the feature space models were used to extract salinization information. The dynamics of land salinization in Tongyu county for the period of 1998 to 2017 were investigated. This research was expected to provide a reference for the methods used for the dynamic monitoring of salinization in the semi-arid Tongyu county, Northeast China. The result may offer scientific evidences for the land management and landscape ecological regulation in this region.

2. STUDY AREA

Tongyu County is in the western fringe of the Songnen Plain, extending from 122°02'13"E-123°30'57"E in longitude and 44°13'57"N-45°16'27"N in latitude (Figure 1). The total land

* Corresponding author

area of the county is 8496 km^2. It belongs to the semi-arid and semi-humid continental monsoon climate in the temperate zone. The average annual temperature is around 4°C, and extreme temperatures ranges from -32 to 38.9°C. The average annual precipitation is 370mm-500mm and rainfall mainly concentrates between June and August (Ren et al., 2010). The average annual evaporation ranges from 900mm to 1000mm owing to an abundant supply of solar energy. The terrain is gentle, with the altitude of 120m-180m. The soil parent materials are quaternary lacustrine sediments and river alluviums. The soil types in Tongyu county include light chernozem soil (Haplic Chernozem, FAO), aeolian sandy soil, meadow soil (Eutric Vertisol, FAO), alkaline soil (Solonetz, FAO), marsh soil, saline soil (Solonchak, FAO) etc. The Huolin River originated in the eastern part of the Greater Xing'an Mountains, scatters between the sandy land and dunes in the northern part of the area, forming the wetland dominated by reed, namely, the Xianghai Wetlands. Due to strong wind and sand, arid climate, and severe water deficit, local agriculture is mainly dryland farming. It has abundant grassland resources and has been approved as the only livestock husbandry dominated county in Jilin province since 1978. Songnen Plain, which is the largest production base of commodity grain in China, with approximately 3.2m ha saline land (21% of the area of the Plain) (Wang et al., 2009).The occurrence of the land salinization in this region results from the natural causes including neo-plate tectonics (Wang et al., 1985), shallow depth groundwater (Song et al., 2000; Zhang et al., 2000) and arid or semiarid climate (Yu et al., 1993; Liu et al., 2002). Human activities are also considered as the main driving factors to the soil salinization (Liu et al., 2005; Huang et al., 2012). In the last several decades, land salinization has been aggravated constantly in the plain (Wang and Li, 2018).

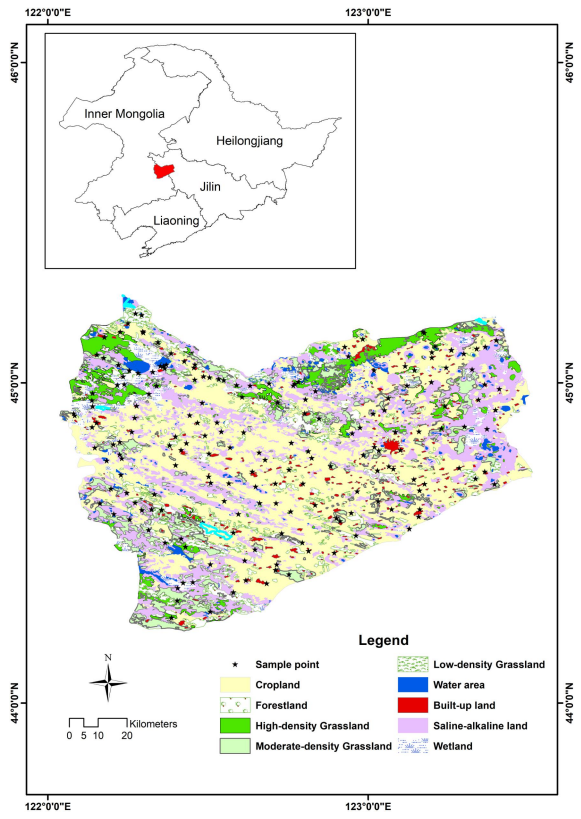

Figure 1. The location and land use of Tongyu county

3. METHOD

3.1 Data Collection and Processing

A Landsat 5 TM image (May 30, 1998) and a Landsat 8 OLI image (May 2, 2017), with a path/row of 120/29, were downloaded from Geospatial Data Cloud website (http://www.gscloud.cn/). The quality of the images was high with a total cloud cover of less than 2%. Atmospheric correction is the process of eliminating the radiation error caused by atmospheric influence and retrieving the true surface reflectance of ground objects (Zheng et al., 2004). The images were atmospherically corrected using the Fast Line-of-sight Atmospheric Analysis of Hypercubes (FLAASH) atmospheric correction tool in ENVI 5.3. These images were intersected with the boundary of Tongyu county to clip out an identical area. The normalized water body index (NDWI), derived from the spectral reflectance in green band and near-infrared band, was calculated to detect and delineate water bodies and wetlands in satellite images.

Auxiliary data of this study included a vector map of Tongyu's administrative division, and the classified map of land cover. The land cover classification data with 30 m resolution was produced using the visual interpretation classification method. 191 topsoil samples were collected at a depth of 0-20 cm from areas with different soil types and vegetation types in 2006 (Ren et al., 2008). Using soil suspension with a water-soil ratio of 5:1, the soil pH was measured by the potentiometric method in the laboratory.

3.2 Construction of Feature Space Model

3.2.1 Feature Space Variables: Previous studies indicated that NDVI could be used as an important index to evaluate desertification, and there existed significant negative correlation between the NDVI and albedo in different desertification areas (Ma et al., 2011; Wei et al., 2018). Different desertification lands could be effectively segmented by dividing the vertical feature space of albedo-NDVI into the change trend of desertification (Verstraete and Pinty, 1996). Similarly, the two-dimensional space composed of salinity index, albedo or vegetation index may be used to extract information regarding salinization.

Albedo is one of the most important parameters of the surface radiation energy balance, which varies among soil moisture, vegetation cover, snow cover, and other land surface conditions. In the absence of irrigation conditions, the humidity of salinized soil near the top soil is greatly affected by groundwater. Relatively high groundwater soils have relatively high moisture levels, and the topsoil has a high salt content. Field verification reveals that the shallower the buried depth of the groundwater is, the greater the soil moisture is. The higher the salinity of the soil is, the lower the surface average albedo is (Ha et al., 2009). Albedo can reveal the information of land salinization in the study area. Albedo were computed as the following formula (Liang et al., 2003):

$$albedo = 0.356\rho_{blue} + 0.13\rho_{red} + 0.373\rho_{nir} + 0.085\rho_{swir1} + 0.072\rho_{swir2} - 0.0018 \quad (1)$$

where ρ_{blue} , ρ_{red} , ρ_{nir} , ρ_{swir1} and ρ_{swir2} is the spectral reflectance in blue, red, near infrared, the shortwave infrared regions, respectively.

By comparing the spectral characteristics and band mixing experiments of typical objects, the soil salinity indices derived

from blue and red bands of remote sensing images can reveal the information of soil salinization (Scudiero et al., 2015). A significant positive correlation between the soil salinity indices and field observed salt content were found. Thus, soil salinity indices were selected as a biophysical parameter for monitoring salinization dynamics. In this present study, the salinity index (SI) was calculated by the following equation (Khan et al., 2001):

$$SI = \sqrt{\rho_{blue} \times \rho_{red}} \tag{2}$$

where ρ_{blue} and ρ_{red} is the spectral reflectance in blue band and red band, respectively.

The remotely sensed vegetation reflectance can be used as an indirect indicator of soil salinity because soil salinity impacts the growth of vegetation (Guo et al., 2019). Salt is one of the most important factors that restricts vegetation growth in soil chemistry (Fan et al., 2015). With the increase of salt content in surface soil, vegetation cover and vegetation index may decrease and the soil electrical conductivity increases accordingly (Wu et al., 2014). MSAVI (modified soil adjusted vegetation index) fully considers the bare soil line and thus effectively eliminates the background influence of soil and vegetation canopy (Weng et al., 2008). The formula for MSAVI was shown as follows (Qi et al., 1994):

$$MSAVI = \frac{(2\rho_{nir}+1) - \sqrt{(2\rho_{nir}+1)^2 - 8(\rho_{nir} - \rho_{red})}}{2} \tag{3}$$

where ρ_{red} and ρ_{nir} is the reflectance in red and near infrared band, respectively.

3.2.2 Data Normalization: To eliminate the differences in magnitude of albedo, salinity index and vegetation index, the maximum and minimum values for these variables were calculated and the data standardization were performed.

$$A = \frac{albedo - albedo_{min}}{albedo_{max} - albedo_{min}} \tag{4}$$

$$S = \frac{SI - SI_{min}}{SI_{max} - SI_{min}} \tag{5}$$

$$M = \frac{MSAVI - MSAVI_{min}}{MSAVI_{max} - MSAVI_{min}} \tag{6}$$

3.2.3 Relationships among Feature Space Variables: To reveal the relationship between multiple feature space variables, we uniformly arranged 300 points in the whole study area, and the corresponding points values of SI, albedo and MSAVI were extracted. SPSS software was used for the statistical regression analysis of the three feature space variables and to investigate their quantitative relations. The feature space models of albedo-SI and MSAVI-SI were constructed, respectively.

3.3 Calculation of Salinization Monitoring Index and Salinization Detection Index

Different desertification lands can be effectively separated by dividing the albedo-NDVI feature space in the vertical direction into changing trends of desertification (Verstraete and Pinty, 1996). Likewise, different salinization lands can be identified by dividing the albedo-SI feature space in the vertical direction into changing trends of salinization. There was an obvious linear relationship between albedo and SI (Figure 2a).

$$albedo = a \times SI + b \tag{7}$$

where a is the slope of the soil line, and b represents the intercept of the soil baseline.

The straight line L, passing through the origin of the coordinate and perpendicular to the soil line is defined. The distance from any point in the albedo-SI feature space to line L can be utilized to explain the soil salinization process. The farther away from the line L, the more serious salinization is. The vertical distance to line L can be calculated by the following formula: (Ha et al., 2009):

$$SMI = \frac{1}{\sqrt{a^2+1}}(SI + a \times albedo) \tag{8}$$

where SMI is defined as the salinization monitoring index, a is the slope of the soil line.

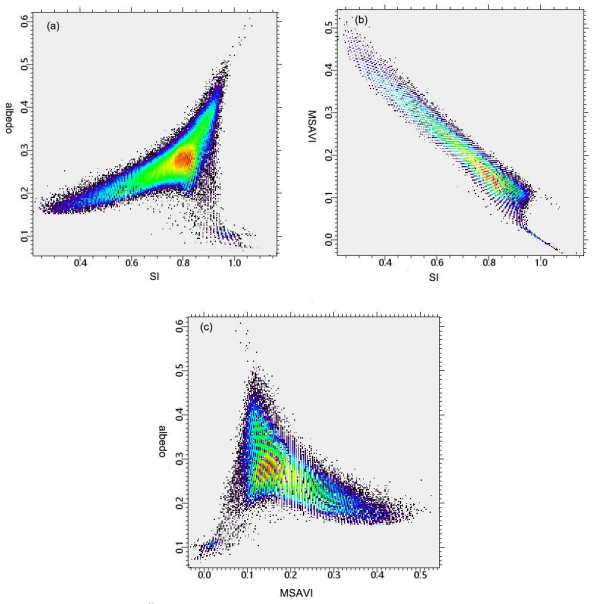

Figure 2. The constructed feature space (a) albedo-SI (b) MSAVI-SI (c) albedo-MSAVI

An obvious negative linear relationship between MSAVI and SI was also observed (Figure 2b,2c). Taking any point in the MSAVI-SI feature space and according to the distance formula between point and line, the remote sensing monitoring model of soil salinization (salinization detection index, SDI) can be expressed as the distance from the point to line L(Guo et al., 2019):

$$SDI = \frac{|1 - MSAVI + M \times SI|}{\sqrt{M^2+1}} \tag{9}$$

where the M represents to the slope of soil line.

4. RESULTS AND DISCUSSION

4.1 Quantitative Relationships among Feature Space Variables

The linear formula and correlation coefficient results of the three feature space variables in 1998 and 2017 are shown in Figure 3 and Figure 4. Here, surface albedo had a significant positive correlation with SI, with correlation coefficient of 0.8572 in 1998 and 0.6324 in 2017, respectively (Figure 3a,4a), while MSAVI had a negative correlation with SI, with correlation coefficient of 0.2981 in 1998 and 0.2525 in 2017, respectively (Figure 3b,4b). The linear relationships between albedo and MSAVI were weak (Figure 3c,4c). Therefore, the three sets of feature space variables with the strongest correlation were selected to construct the feature space models of albedo-SI and MSAVI-SI, respectively.

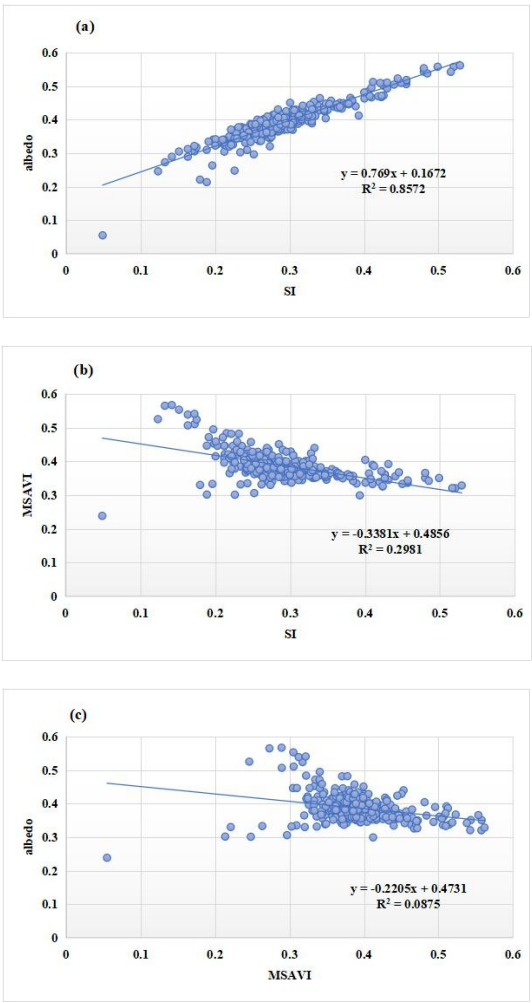

Figure 3. Correlation between variables of different eigenspaces in 1998: (a) albedo-SI (b) MSAVI-SI (c) albedo-MSAVI

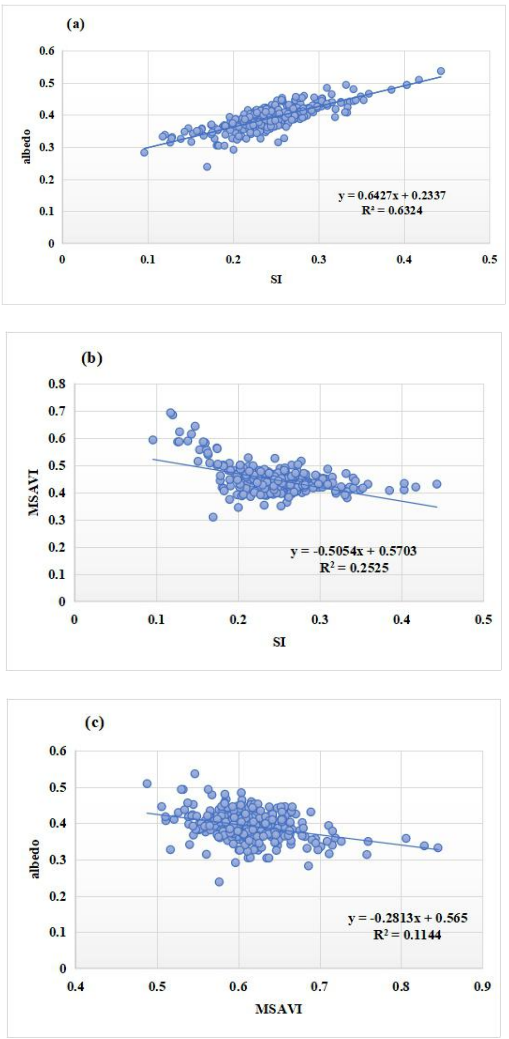

Figure 4. Correlation between variables of different eigenspaces in 2017: (a) albedo-SI (b) MSAVI-SI (c) albedo-MSAVI

4.2 Changes of Feature Space Variables

Spatial characteristic of three feature space variables (albedo, MSAVI and SI) in Tongyu county in 1998 and 2017 are shown in Figure 5 and Figure 6, respectively. From 1998 to 2017, the three feature space variables changed differently. The regional average albedo decreased from 0.175 to 0.169 during the past 20 years. By comparison, average MSAVI increased by 0.1. Regarding the average SI, the values were 0.104 in 1998 and 0.063 in 2017, respectively. The maximum values of albedo were almost unchanged. The MSAVI maximum value increased from 0.722 to 0.815, while the maximum value of SI decreased from 0.577 to 0.429.

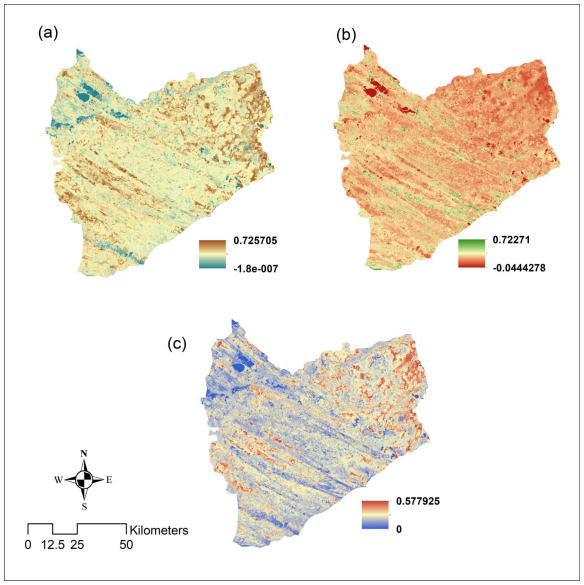

Figure 5. Spatial pattern of albedo(a) MSAVI(b) SI(c) in 1998

The spatial distribution of three feature space variables was generally consistent with the land cover type. Woodland refers to bushes, shrubs, and forest. The regions covered by forests showed highest MSAVI, but had low albedo and SI. The SI and albedo mean value of saline-alkaline land ranked first, whereas MSAVI was lower. During 1998-2017, the average SI value of saline-alkaline land decreased by 45%, and MSAVI increased from 0.144 to 0.31. Grassland is the area used for grazing that can be degraded by overgrazing and waterlogging. The average SI of grasslands decreased by 0.062, suggesting the salinization tended to improve. The average SI value of cropland decreased from 0.158 in 1998 to 0.097 in 2017, while average MSAVI increased from 0.168 to 0.343, respectively.

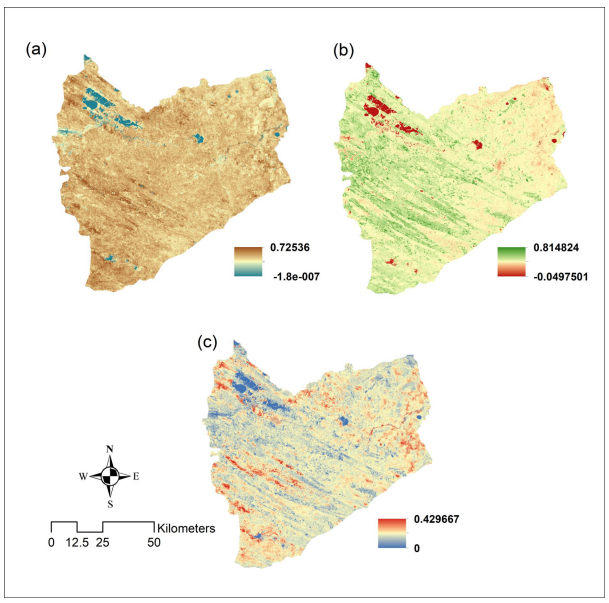

Figure 6. Spatial pattern of (a) albedo(b) MSAVI (c) SI in 2017

4.3 Land Salinization Dynamic over 1998-2017

The feature space models of albedo-SI and MSAVI-SI for Tongyu county in 1998 and 2017 were constructed. The SMI and SDI were then calculated and their values were divided into five different levels by the natural break (Jenks) classification. The natural break classification method is based on natural grouping inherent in the data, whose boundary is set to the position where the data values are relatively different (Zeng et al., 2013). The method calculates each kind of classifications, and automatically selects the classification situation with the minimum variance, thereby the optimal classification result can be obtained. Moreover, similar classes can be effectively merged and the differences between classes may be maximized. The five salinization levels in Tongyu county were severe salinization, high salinization, medium salinization, low salinization, and non salinization.

Table 1 indicates the ranges of salinization monitoring index (SMI) and salinization detection index (SDI) values for Tongyu county. In the severe salinization areas, there showed the highest albedo and SI values, but had the lowest MNDVI values with almost no vegetation coverage. By contrast, the non-salinization areas covered by vegetation had the lowest albedo and SI values. Figure 7 and Figure 8 illustrate the spatial distribution of land salinization degree derived from SMI and SDI in 1998 and 2017, respectively. According to SMI, most of severe/high salinization were found in the northeast or southwest parts of Tongyu county in 1998, whereas severe/high salinization land defined by SDI showed more extensive distribution (Figure 7a and 8a). Spatially, severe saline-alkali lands presented an agglomeration distribution. In 2017, the areas of severe/high salinization land dropped dramatically, showing scattered distribution. Medium salinization lands extracted from SMI dominated in the study area (Figure 7b), while the areas of low salinization derived from SDI were the largest (Figure 8b).

Land Salinization Index	Level	Value
SMI	Non salinization	<0.17
	Low salinization	0.17-0.29
	Medium salinization	0.29-0.37
	High salinization	0.37-0.45
	Severe salinization	>0.45
SDI	Non salinization	0
	Low salinization	0-0.56
	Medium salinization	0.56-0.62
	High salinization	0.62-0.68
	Severe salinization	>0.68

Table 1. The ranges of salinization monitoring index (SMI) and salinization detection index (SDI) values for land salinization at different levels.

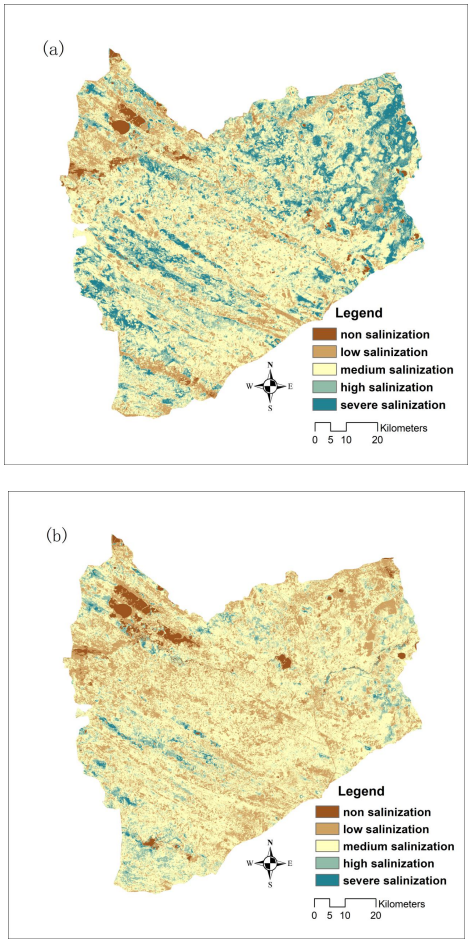

Figure 7. Spatial pattern of land salinization based on SMI in Tongyu county (a) 1998 (b) 2017

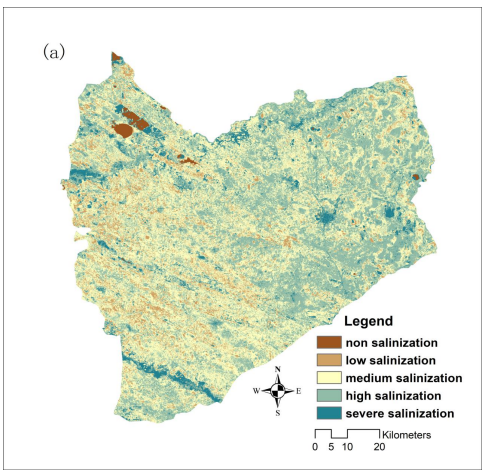

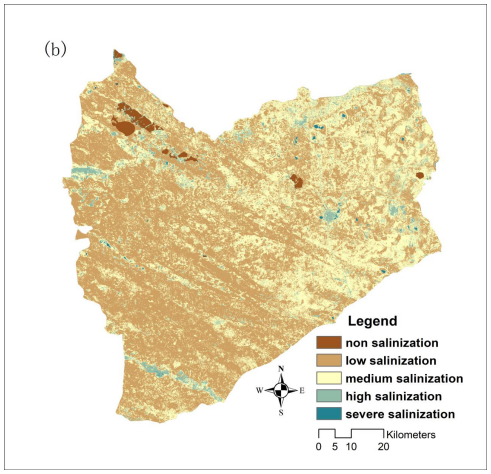

Figure 8. Spatial pattern of land salinization based on SDI in Tongyu county (a) 1998 (b) 2017

Level	SMI (area %)		SDI (area%)	
	1998	2017	1998	2017
Non salinization	1.68	2.28	0.72	1.08
Low salinization	19.38	28.12	8.44	81.41
Medium salinization	49.56	60.84	43.44	16.15
High salinization	19.64	7.79	41.49	1.12
Severe salinization	9.74	0.96	5.91	0.24

Table 2. Changes in area percentages of different salinization accounting for the total land, derived from albedo-SI and MSAVI-SI.

The area percentages of land salinization accounting for the total landscape differed based on the feature space model used, as shown in Table 2. Table 2 represents the statistics of the extraction results regarding salinization in the year of 1998 and 2017. One of the most noticeable change is the shrinkage in land salinization over the 20-year study period. The difference between the two methods is that the high salinization areas extracted by MSAVI-SI were larger in 1998, while the non-salinization, low, medium and severe salinization areas were smaller than those extracted by the albedo-SI model. In 2017, the medium salinization areas extracted by albedo-SI were larger than those extracted by the MSAVI-SI model. The area percentages of severe and high salinization land based on SMI declined by 8.78% and 11.85%, whereas medium and low salinization land increased by 11.28% and 8.74%, respectively. The area percentages of severe, high and medium salinization based on SDI dropped by 5.67%, 40.37% and 27.29%. In contrast, the area of low salinization land accounting for the total area increased 72.97%. The highly and severely salinized areas decreased overall, which may owe to the effectiveness of mechanical, biological, ecological, and engineering measurements for rehabilitation of irreversibly degraded lands in this county.

To examine the accuracy of the land salinization monitoring models, the corresponding SMI and SDI values of field sample points were extracted from the two indices images. The pH measurements of 191 samples were used to established the the fitting relationship with two land salinization indices. To approximately match the collection time of soil samples, we used the Landsat 5 TM image in 2007 to calculate the SMI and SDI. As shown in Figure 9, the determination coefficient (R^2)

between SMI and soil pH was higher (0.3344), indicating that the inversion accuracy of the albedo-SI feature space with SMI was higher than the MSAVI-SI with SDI. Therefore, the remote sensing monitoring model based on albedo-SI with SMI was the more effective approach to obtain the information of saline soil in the Tongyu county.

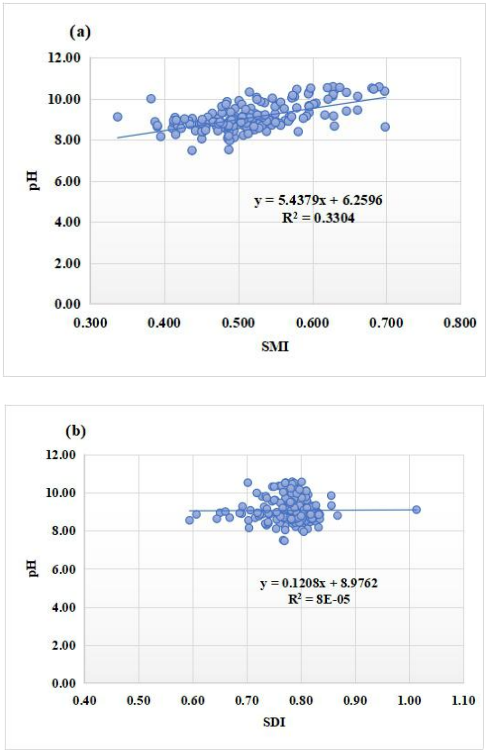

Figure 9. Comparisons of inversion accuracy for different monitoring models (a) SMI (b) SDI.

5. CONCLUSIONS

Based on Landsat TM and OLI images, albedo, typical vegetation indices (MSAVI) and the salinity index (SI) were calculated and selected to construct two feature space (albedo-SI and MSAVI-SI) models. Using the salinization monitoring index and detection index (SMI and SDI) derived from the feature space models, land salinization information in 1998 and 2017 for Tongyu county, Northeast China were extracted. It was found that land salinization over the 20-year study period has undergone a process of improvement. Severe and high salinization land decreased significantly. It is more feasible to extract salinization information using the feature space model of albedo-SI.

ACKNOWLEDGEMENTS

The authors would like to acknowledge the Project 41571405 supported by National Natural Science Foundation of China.

REFERENCES

Allbed, A., Kumar, L., Aldakheel, Y.Y., 2014. Assessing soil salinity using soil salinity and vegetation indices derived from IKONOS high-spatial resolution imageries: applications in a date palm dominated region. *Geoderma*, 230-231,1-8. doi.org/10.1016/j.geoderma.2014.03.025.

Ding, J.L., Qu, J., Sun, Y.M., Zhang, Y.F., 2013. The retrieval model of soil salinization information in arid region based on MSAVI-WI feature space: a case study of the delta oasis in WeiganKuqa watershed. *Geographical Research*, 32(2),223-232. doi.org/10.11821/yj2013020003.

Ding, J.L., Yu, D.L., 2014. Monitoring and evaluating spatial variability of soil salinity in dry and wet seasons in the Werigan–Kuqa Oasis, China, using remote sensing and electromagnetic induction instruments. *Geoderma*, 235-236(4), 316-322. doi.org/10.1016/j.geoderma.2014.07.028.

Fan, X.W., Liu, Y.B., Tao, J.M., Weng, Y.L., 2015. Soil salinity retrieval from advanced multi-Spectral sensor with partial least square regression. *Remote Sensing*,7(1),488-511. doi.org/10.3390/rs70100488.

Gao, J., Liu, Y.S., 2010. Determination of land degradation causes in Tongyu county, Northeast China via land cover change detection. *International Journal of Applied Earth Observation and Geoinformation*, 12(1),9-16. doi.org/10.1016/j.jag.2009.08.003.

Gu, H. B., Song, Y., Pan, J., 2010. Research progress of influencing factors on salinization of Songnen Plain. *Journal of Anhui Agricultural Science*, 38(30), 95-98.

Guo, B., Han, B. M., Yang, F., Fan, Y. W., Jiang, L., Chen, S. T., Yang, W. N., Gong, R., Liang, T., 2019. Salinization information extraction model based on VI–SI feature space combinations in the Yellow River Delta based on Landsat 8 OLI image, *Geomatics, Natural Hazards and Risk*, 10(1), 1863-1878. doi.org/10.1080/19475705.2019.1650125.

Ha, X. P., Ding, J. L., Tashpolat,T., Gao, T. T., Zhang, F., 2009. SI-Albedo Space-based Remote Sensing Synthesis Index Models for Monitoring of Soil Salinization, *Acta Pedologica Sinica*, 46(4), 698-703.

Huang, F., Wang, P., Zhang, J.J., 2012.Grasslands changes in the Northern Songnen Plain, China during 1954-2000. *Environ Monit Assess*, 184(4), 2161-2175. doi.org/10.1007/s10661-011-2107-6.

Khan, N. M., Sato, Y., 2001. Monitoring hydro-salinity status and its impact in irrigated semi-arid areas using IRS-1B LISS-II data. *Asian Journal of Geo informatics*, 1(3), 63-73.

Liang, S.L,, Shuey, C.J., Russ, A.L., Fang, H., Chen, M.,Walthall, C.L., Daughtry, C.S.T., Hunt, R., Jr. 2003.Narrowband to broadband conversions of land surface albedo: II. Validation. *Remote Sensing of Environment*, 84(1), 25-41. doi.org/10.1016/S0034-4257(02)00068-8.

Line,J. G., Finlaysonc, C. M., Falkenmark, M., 2010. Managing water in agriculture for food production and other ecosystem services. *Agricultural Water Management*, 97(4), 512-519. doi.org/10.1016/j.agwat.2009.03.017.

Liu, G. M., Yang, J. S., Li, D. S., 2002. Evaporation regularity and its relationship with soil salt. *Acta Pedologica Sinica*,39 (3), 384-389.

Liu, Q., He, Y., Deng, W., Zhang, G.X., 2005. Study on the soil salinization process in the changeable environment: A case

study in the middle and lower reaches of Taoer River. *Journal of Arid Land Resources and Environment*, 19(6), 113-117.

Ma, Z., Xie, Y., Jiao, J., Wang, X., 2011.The Construction and Application of an Aledo-NDVI Based Desertification Monitoring Model. *Procedia Environmental Sciences*, 10, 2029-2035. doi.org/10.1016/j.proenv.2011.09.318.

Masoud, A. A., Koike, K., 2006. Arid land salinization detected by remotely-sensed land cover changes: A case study in the Siwa region, NW Egypt. *Journal of Arid Environments*, 66(1), 151-167. doi.org/10.1016/j.jaridenv.2005.10.011.

McFeeters,S. K., 1996. The use of the Normalized Difference Water Index (NDWI) in the delineation of open water features. *International Journal of Remote Sensing*, 17(7),1425-1432. doi.org/10.1080/01431169608948714.

Peng, J., Biswas, A., Jiang, Q.S., Zhao, R.Y., Hu, J., Hu, B.F., Shi, Z., 2019. Estimating soil salinity from remote sensing and terrain data in southern Xinjiang Province, China. *Geoderma*, 337,1309-1319. doi.org/10.1016/j.geoderma.2018.08.006.

Qi, J., Chehouni, A., Huete, A.R., Kerr, Y.H., Sorooshian, S.,1994. A modified soil adjusted vegetation index. *Remote Sens. Environ.* 48(2), 119-126. doi.org/10.1016/0034-4257(94)90134-1.

Ren, C. Y., Zhang, B., Wang, Z. M., Song, K. S., Liu, D. W., 2010. Analysis of land use change and its driving forces in the farming-pastoral ecotone of western Songnen Plain:a case study of Tongyu county, Jilin Province. *Journal of Arid Land Resources and Environment*, 24(6), 96-102.

Ren, C. Y., Zhang, B., Wang, Z. M., Song, K. S., Liu, D. W., 2008. Study on spatial variability of soil organic carbon content in the West Songnen Plain:a case study Tongyu county, Jilin province. *Arid Zone Research*, 25(5), 630-636.

Scudiero, E., Skaggs, T.H., Corwin, D.L.,2015. Regional-scale soil salinity assessment using Landsat ETM+ canopy reflectance. *Remote Sensing of Environment*, 169, 335-343. doi.org/10.1016/j.rse.2015.08.026.

Song, C. C., Deng, W., 2000. Characters of groundwater and influence on the interior salt-affected soil in the west of Jilin province. *Scientia Geographica Sinica*, 20(3), 246-230.

UNEP, 1991. Status of desertification and implementation of the United Nations plan of action to combat desertification. Nairobi, Kenya.

Verstraete, M. M., Pinty, B., 1996. Designing optimal spectral indexes for remote sensing applications. *IEEE Transactions on Geoscience and Remote Sensing*, 34(5),1254-1265. doi.org/10.1109/36.536541.

Wang, L, Seki, K., Miyazaki, T., *et al*., 2009. The causes of soil alkalinization in the Songnen Plain of Northeast China. *Paddy and Water Environment*, 7(3), 259-270.doi.org/10.1007/s10333-009-0166-x.

Wang, Z. X., Su, Q. S., Lin ,S. Z. Zhang,Q.Y., Cao, Y.Q., 1985. Groundwater and Quaternary Geology at Baicheng. Beijing: Geological Publishing House.

Wang, Z .Y., Li, L. J., 2018. Determination of land salinization causes via land cover and hydrological process change detection in a typical part of Songnen Plain. *Journal of Geographical Sciences*, 28(8), 1099-1112. doi.org/10.1007/s11442-018-1544-3.

Wei, H. S., Wang, J. L.,Cheng, K., Li,G., Ochir,A., Davaasuren, D.,Chonokhuu, S., 2018. Desertification information extraction based on feature space combinations on the Mongolian Plateau. *Remote Sensing,* 10, 1614, doi.org/10.3390/rs10101614.

Weng, Y.L., Gong, P., Zhu, Z.L., 2008. Soil salt content estimation in the Yellow River delta with satellite hyperspectral data. *Canadian Journal of Remote Sensing*, 34(3),259-270. doi.org/10.5589/m08-017.

Wu, W., Mhaimeed, A.S., Al-Shafie, W.M., Ziadat, F., Dhehibi, B., Nangia, V., De Pauw, E., 2014. Mapping soil salinity changes using remote sensing in Central Iraq. *Geoderma Regional*, 2-3:21-31. doi.org/10.1016/j.geodrs.2014.09.002.

Yu, R. P., You, W. R., 1993. Monitor and Prevention of Salt-affected Soil. Beijing: Science Press.

Wu, Z.H., Tao, L.I., 2013. The comprehensive performance evaluation of the high-tech development zone:Analysis based on the natural breakpoint method. *Statistics and Information Forum*, 3, 82-88.

Zhang, D. F., 2000. Study on soil salinization in the Western Plain of Jilin Province based on GIS. Changchun: Changchun University of Science and Technology.

Zhang, T. Y., Wang, L., Zeng, P.L., Wang, T., Geng, Y.H., Wang, H., 2016. Soil salinization in the irrigated area of the Manas River basin based on MSAVI-SI feature space. *Arid Zone Research*, 33(3), 499-505.

Zheng, W., Zeng, Z.Y., 2004. A Review on Methods of Atmospheric Correction for Remote Sensing Images. *Remote Sensing Information*, 4,66-70.

Revised April 2020